Year: 2021

Biogeography of the monocotyledon astelioid clade (Asparagales): A history of long-distance dispersal and diversification with emerging habitats

Birch, Joanne L ; Kocyan, Alexander

Abstract: The astelioid families (Asteliaceae, Blandfordiaceae, Boryaceae, Hypoxidaceae, and Lanariaceae) have centers of diversity in Australasia and temperate Africa, with secondary centers of diversity in Afromontane Africa, Asia, and Pacific Islands. The global distribution of these families makes this an excellent lineage to test if current distribution patterns are the result of vicariance or long-distance dispersal and to evaluate the roles of tertiary climatic and geological drivers in lineage diversification. Sequence data were generated from five chloroplast regions (petL-psbE, rbcL, rps16-trnK, trnL-trnLF, trnS-trnSG) for 104 ingroup species sampled across global diversity. The astelioid phylogeny was inferred using maximum parsimony, maximum likelihood, and Bayesian inference methods. Divergence dates were estimated with a relaxed clock applied in BEAST. Ancestral ranges were reconstructed in 'BioGeoBEARS' applying the corrected Akaike information criterion to test for the best-fit biogeographic model. Diversification rates were estimated in Bayesian Analysis of Macroevolutionary Mixtures [BAMM]. Astelioid relationships were inferred as Boryaceae(Blandfordiaceae(Asteliaceae(Hypoxidaceae plus Lanariaceae))). The crown astelioid node was dated to the Late Cretaceous (75.2 million years; 95% highest posterior densities interval 61.0-90.0 million years) with an inferred Eastern Gondwanan origin. However, astelioid speciation events have not been shaped by Gondwanan vicariance. Rather long-distance dispersal since the Eocene is inferred to account for current distributions. Crown Asteliaceae and Boryaceae have Australian ancestral ranges and diversified since the Eocene. In Hypoxidaceae, Empodium, Hypoxis, and Pauridia have African ancestral ranges; Curculigo and Molineria have an Asian ancestral range and have diversified since the mid-Miocene. Diversification of Pauridia and the Curculigo clade has occurred steadily, while diversification of Astelia and Hypoxis was punctuated over time. Diversification of those genera coincides temporally with the expansion of the habitat types occupied by extant taxa, e.g., grassland habitat in Africa during the late Miocene and alpine habitat in New Zealand during the Pliocene.

Originally published at:

Biogeography of the monocotyledon astelioid clade (Asparagales): A history of long-distance dispersal and diversification with emerging habitats

Joanne L. Birch [a,b,*], Alexander Kocyan [c,d,*]

[a] *University of Melbourne, School of BioSciences, Parkville, VIC 3010, Australia*
[b] *University of Hawai'i at Mānoa, Department of Botany, Honolulu, Hawai'i 96822, USA*
[c] *University of Zurich, Department of Plant and Microbial Biology, Botanical Museum, Zollikerstrasse 107, 8008 Zurich, Switzerland*
[d] *University of Potsdam, Institute of Biochemistry and Biology, Biodiversity Research/Systematic Botany, Maulbeerallee 2a, 14469 Potsdam, Germany*

ARTICLE INFO

ABSTRACT

The astelioid families (Asteliaceae, Blandfordiaceae, Boryaceae, Hypoxidaceae, and Lanariaceae) have centers of diversity in Australasia and temperate Africa, with secondary centers of diversity in Afromontane Africa, Asia, and Pacific Islands. The global distribution of these families makes this an excellent lineage to test if current distribution patterns are the result of vicariance or long-distance dispersal and to evaluate the roles of Tertiary climatic and geological drivers in lineage diversification. Sequence data were generated from five chloroplast regions (*petL-psb*E, *rbc*L, *rps*16-*trn*K, *trn*L-*trn*LF, *trn*S-*trn*SG) for 104 ingroup species sampled across global diversity. The astelioid phylogeny was inferred using maximum parsimony, maximum likelihood, and Bayesian inference methods. Divergence dates were estimated with a relaxed clock applied in BEAST. Ancestral ranges were reconstructed in the R package 'BioGeoBEARS' applying the corrected Akaike information criterion to test for the best-fit biogeographic model. Diversification rates were estimated in Bayesian Analysis of Macroevolutionary Mixtures (BAMM). Astelioid relationships were inferred as Boryaceae(Blandfordiaceae(Asteliaceae (Hypoxidaceae plus Lanariaceae))). The crown astelioid node was dated to the Late Cretaceous (75.2 million years; 95% highest posterior density interval 61.0–90.0 million years) and an Antarctic-Australasian origin was inferred. Astelioid speciation events have not been shaped by Gondwanan vicariance. Rather long-distance dispersal since the Eocene is inferred to account for current distributions. Crown Asteliaceae and Boryaceae have Australian ancestral ranges and diversified since the Eocene. In Hypoxidaceae, *Empodium*, *Hypoxis*, and *Pauridia* have African ancestral ranges, while *Curculigo* and *Molineria* have an Asian ancestral range. Diversification of *Pauridia* and the *Curculigo* clade occurred steadily, while diversification of *Astelia* and *Hypoxis* was punctuated over time. Diversification of *Hypoxis* and *Astelia* coincided temporally with the expansion of the habitat types occupied by extant taxa, e.g., grassland habitat in Africa during the Late Miocene and alpine habitat in New Zealand during the Pliocene, respectively.

1. Introduction

Taxon-centered studies can shed light on the timing of past diversification, the tempo of species accumulation (Linder et al., 2003; Crisp et al., 2004), and the processes driving diversification of lineages (Verboom et al., 2003; Gunn et al., 2020). For globally distributed lineages, comparison of diversification among continental floras can provide insights into the comparative influences of global and regional climatic, geologic, and edaphic factors on biome evolution (Crisp et al., 2004),

vegetation change (Bouchenak-Khelladi et al., 2010), and community assembly (Carpenter et al., 2015; Tanentzap et al., 2015).

The Asparagales is the largest monocotyledon order with ca. 36,265 species (Stevens 2001 onwards). It is morphologically and ecologically diverse, including the megadiverse Orchidaceae Juss. (ca. 22,000 species) and many smaller, but economically (e.g. *Asparagus* L., *Allium* L.) and ecologically (e.g. *Xanthorrhoea* Sol ex Sm., *Hypoxis* L.) significant taxa. Large scale monocotyledon studies have consistently placed Orchidaceae sister to the rest of the Asparagales, with an astelioid clade

sister to a clade containing all the remaining Asparagales lineages (Givnish et al., 2006; Pires et al., 2006; Seberg et al., 2012). The Asparagales are estimated to have diversified within the Cretaceous, between approximately 120–105 million years ago (Ma) (Bell et al., 2010; Uribe-Convers et al., 2017; Givnish et al., 2018) with a proposed center of origin in West Gondwana (Raven and Axelrod, 1974) or Australasia (Bremer and Janssen, 2006) and significant diversity in Africa (Wiland-Szymańska, 2001; Singh, 2009).

The astelioid clade includes five primarily Southern Hemisphere families (Asteliaceae, Blandfordiaceae, Boryaceae, Hypoxidaceae, Lanariaceae) in 15 genera and ca. 210 species. Astelioid taxa are present globally, except in Europe, with Australian (Blandfordiaceae, Boryaceae), Austral-Pacific (Asteliaceae), and African (Hypoxidaceae, Lanariaceae) centers of diversity (Fig. 1). Raven and Axelrod (1974) considered that the family distributions reflect a "history of long-standing connections between Africa and Australasia", though they noted that "it is difficult to say why if they are so old they are so poorly represented in South America".

To-date, astelioid biogeographic studies have focused on generic diversity. *Astelia* has undergone recent, long-distance dispersal to Pacific and Indian Ocean islands, as well as between New Zealand and Australia and, independently, South America (Birch and Keeley, 2013). However, sampling did not enable determination of the role of vicariance on family diversification (Birch et al., 2012). The timing of diversification of Hypoxidaceae taxa has not yet been estimated. Within Hypoxidaceae, the most species rich genus, *Hypoxis*, is considered a component of an Afromontane (White, 1981) element of the African flora and its diversification is proposed to be linked to the expansion of grasslands on the continent as a result of climate change (Singh, 2009).

Provision of a temporal scale for diversification can provide insights into the response of lineages to habitat change associated with geologic or climatic conditions. Gondwanan floras experienced warm and humid conditions until the Early Eocene (Zachos et al., 2001). Against a global backdrop of a cooling Tertiary climate, all Gondwanan floras have experienced episodes of higher rates of cooling during the Late Eocene to Early Oligocene (ca. 34 Ma), the Middle Miocene (ca. 15–14 Ma), and the Late Pliocene (ca. 3 Ma) (Zachos et al., 2001; Lewis et al., 2008). If global climatic conditions affected the diversification of these lineages, the diversification of both temperate and tropical lineages should reflect these climatic changes. Of particular interest, in terms of the habitat occupancy of astelioid taxa, is the presence of arid- and mesic-adapted taxa as well as forest and grassland associated taxa. Therefore, astelioids hold potential to understand the impacts of increasing global aridification from the Middle Miocene onwards (Byrne et al., 2011; van Zinderen Bakker and Mercer, 1986) and of regional geological events, such as tectonic uplift resulting in the expansion of alpine habitats in Australia from the Late Eocene to Pliocene (Holdgate et al., 2008).

Estimation of the time frame of lineage diversification allows identification of factors that might have driven the apparent differential speciation or extinction in these lineages. Range size and species richness vary extensively in astelioid genera. Asteliaceae contains two endemic Australian genera: *Neoastelia*, a monotypic genus of temperate rainforests in central eastern Australia and *Milligania* (5 species), a Tasmanian endemic with taxa occupying lowland, alluvial to alpine herbfield vegetation. Conversely, *Astelia* (30 species; Birch, 2015), the largest genus in the family, has a center of diversity in New Zealand, with secondary centers of diversity in Australia and Hawai'i, and two exceptional occurrences in Africa (La Réunion, Mauritius) and in South America (Patagonia). Blandfordiaceae and Boryaceae are Australian endemics containing a single genus *Blandfordia* (4 species) and *Borya* (13 species) and the monotypic genus *Alania*, respectively. A similar pattern of variable range size and species richness is found in the Hypoxidaceae and Lanariaceae, which have centers of diversity in Africa. Lanariaceae, a monotypic family, is endemic to South Africa where it is found in renosterveld vegetation. Conversely, Hypoxidaceae, contains 8 genera and ca. 160 species with a global distribution (Stevens, 2001). Similar
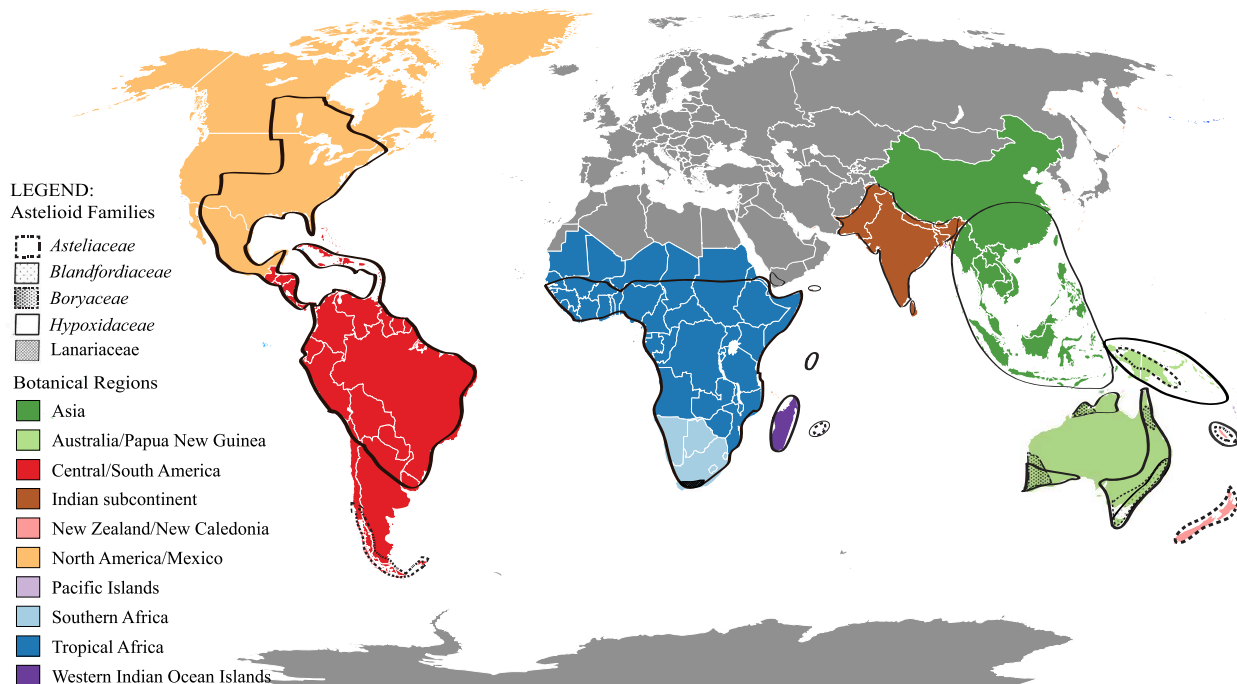

Fig. 1. Global distributions of astelioid families (Asteliaceae, Blandfordiaceae, Boryaceae, Hypoxidaceae, and Lanariaceae) and geographic regions as applied in ancestral range reconstruction analyses. Geographic regions were defined as: Asia; Australia and Papua New Guinea; Central and South America; the Indian subcontinent; New Zealand and New Caledonia; North America and Mexico; Pacific Islands including the Austral Islands, Fiji, Hawai'i, the Marquesas Islands, Samoa, the Society Islands, and Vanuatu; Southern Africa; Tropical Africa, excluding Madagascar, the Mascarene, and the Seychelles Islands; and Western Indian Ocean Islands, including Madagascar, the Mascarene, and the Seychelles Islands. Geographic regions conformed to regions recognized in the World Geographical Scheme for Recording Plant Distributions (Brummitt, 2001). The occupancy of *Astelia* (Asteliaceae) on the Austral Islands, Hawai'i, Samoa, and the Society Islands were not mapped.

patterns are observed in Hypoxidaceae genera; *Hypoxis*, the largest genus, (ca. 90–100 species) and *Curculigo* and *Molineria* (taxonomic circumscriptions of both genera unclear, together 16 species) have global distributions, *Pauridia* (35 species; Snijman and Kocyan, 2013) and *Empodium* (8 species) have centers of diversity in the winter rainfall region of southern Africa, and smaller genera include *Rhodohypoxis* (2 species), which is native to southern Africa and *Hypoxidia* (2 species) and *Neofriedmannia* (monotypic), which are endemic to the Seychelles Islands.

A phylogeny with representative sampling across all astelioid genera was reconstructed and divergence dates and ancestral ranges were estimated for the clade. This study sought to investigate the following questions: 1. When did astelioid genera diversify and what was the role of vicariance and/or dispersal in determining the distributions of extant taxa, 2. what were the geological and climatic drivers of diversification in Australasian, African, and Asian astelioid lineages, and 3. what factors influencing diversification may have contributed to the variable species richness of astelioid genera.

2. Materials and methods

2.1. Taxon sampling, DNA extraction, PCR, sequencing

One hundred and fourteen ingroup individuals of 104 species representing all currently accepted genera in Asteliaceae, Blandfordiaceae, Boryaceae, Hypoxidaceae, and Lanariaceae were included. We included outgroup taxa from the monocotyledon orders Arecales, Asparagales, Commelinales, Liliales, and Zingiberales (Appendix 1).

For this study 273 sequences were newly generated (Appendix 1) and combined with sequence data from our previous studies (Kocyan et al., 2011; Birch et al., 2012). In short, *pet*L-*psb*E and *rps*16-*trn*K were sequenced for Hypoxidaceae and Lanariaceae and *trn*S-*trn*SG and *rbc*L were sequenced for Asteliaceae. Primers, PCR amplification, and sequencing protocols for *rbc*L, *trn*L-*trn*LF (Hypoxidaceae and Lanariaceae) (hereafter referred to as *trn*LF) and *trn*S-*trn*SG (hereafter referred to as *trn*SG) are detailed in Kocyan et al. (2011) and for *pet*L-*psb*E, *rps*16-*trn*K, and *trn*LF (Asteliaceae) in Birch et al. (2012). Sequence and alignment editing were as explained in those studies.

2.2. Phylogenetic analyses

Phylogenetic reconstructions were completed for individual and combined datasets using the parsimony criterion in PAUP 4.0a (build 166) (Swofford, 2002), maximum likelihood (ML) in RAxML version 8 (Stamatakis, 2014), and Bayesian inference (BA) in MrBayes v 3.2.1 (Ronquist et al., 2012). Congruence of individual markers was assessed visually considering only those nodes with support greater than 65% bootstrap or 0.95 posterior probability values, respectively. Gaps were treated as missing data in all analyses.

Parsimony analysis (MP) and calculation of bootstrap percentages (BP$_P$) were performed as outlined in Birch et al. (2012). For ML and BA analyses of each dataset the best-fit model of evolution was selected based on the corrected Akaike information criterion implemented in the modelTest (Guindon and Gascuel, 2003; Posada, 2008) function in 'phangorn' version 1.99.14 (Schliep, 2011) in R-studio version 1.1.447 (RStudio Team, 2016) (Table 1). Data partitions were identified in PARTITIONFINDER Version 1.1.1 (Lanfear et al., 2016). Maximum likelihood reconstructions were based on the partitioned dataset and were completed as outlined in Birch et al. (2012). Nonparametric bootstrap values (BP$_{ML}$) were calculated with 1000 replicates using the rapid bootstrap algorithm. For BA the dataset was partitioned with models of evolution and parameters applied to or estimated for each partition accordingly. Bayesian analyses were run with two independent replicates of four Markov chains (one heated and three cold) and were run for six million generations and sampled every 6000 generations. Convergence was determined based on an average standard deviation of split frequencies of <0.01. Trees generated during a burn-in period of 1.5 million generations were discarded prior to construction of the 50% maximum consensus trees that were visualized in FIGTREE v1.3.1 (http://tree.bio.ed.ac.uk/software/figtree/). Posterior probabilities (PP) were calculated. BA and ML analyses were run on the Spartan High-Performance Computing system operated by Research Platform Services at the University of Melbourne.

2.3. Divergence dating

Divergence dates were estimated in BEAST 2.6 (Bouckaert et al., 2014). Within Hypoxidaceae the (*Pauridia* + *Empodium*)(*Curculigo* + *Molineria* + *Neofriedmannia* + *Hypoxidia*) clade was constrained to monophyly following the maximum parsimony topology. Divergence date estimates applied a relaxed clock with uncorrelated rates drawn from a lognormal distribution, based on rejection (P < 0.05) of the hypothesis of clock-like molecular evolution for each dataset using likelihood ratio tests conducted in PAUP 4.0a (build 168) (Swofford, 2002). The dataset was partitioned with parameters estimated for each molecular marker and the GTR + Γ model of evolution was applied to each data partition. A Yule speciation tree prior was applied as that model showed a significantly better fit to the data than the birth-death model in a test of the maximum likelihood tree (with the sampling fraction of 0.512 calculated for these data) conducted in the R package 'phytools' (Revell 2012). An MCMC analysis of 300 million generations was performed with sampling every 30,000 generations. A maximum-credibility tree was constructed from 7501 trees after 2500 trees generated during the burn-in period were discarded. Parameters were checked using TRACER 1.6.1 (Rambaut and Drummond, 2007).

We reviewed the monocotyledon fossil and dating literature (including Bell et al., 2010; Iles et al., 2015; Givnish et al., 2018) to identify the most appropriate data (dates and distributions) to serve as a secondary constraint for the basal node of the tree. We assigned a uniform distribution to the Asparagales crown node with date constraints drawn from Givnish et al. (2018; 121.32–111.32 Ma). A prior of 26.0 Ma was applied to the *Astelia* crown node based on Middle Oligocene *Astelia* pollen fossils and Early Miocene leaf cuticle fossils representing the earliest unequivocally determined *Astelia s.l.* fossil records, as outlined in Birch and Keeley (2013). The *Astelia* crown node was assigned a lognormal distribution (mean = 1; standard deviation = 1.0; offset =

Table 1

Descriptive parameters for plastid data sets, parsimony, maximum likelihood, and Bayesian inference reconstructions.

	Number of terminals	Missing data (%)	Aligned length	Parsimony informative characters	Tree length	Number of optimal length trees generated in heuristic search	Retention Index /Consistency Index/Rescaled Consistency Index	Model of evolution
*pet*L-*psb*E	102	18.7	1892	506	1974	714,000	0.72/0.84/0.60	GTR + G + I
*rbc*L	121	7.8	1323	216	878	3,660	0.53/0.83/0.44	GTR + G + I
*rps*16-*trn*K	103	9.0	1112	422	1600	515,000	0.66/0.87/0.57	GTR + G
*trn*L-*trn*LF	118	7.4	1290	337	1321	250	0.66/0.83/0.55	GTR + G + I
*trn*S-*trn*SG	108	5.2	969	340	1325	852,000	0.69/0.89/0.62	GTR + G
Combined	127	28.4	6586	1821	7178	972,000	0.66/0.85/0.56	GTR + G + I

24.0), representing a median of 26.7 Ma, a hard lower (minimum) bound of 24.5 Ma and a soft upper (maximum) bound (95% highest posterior density [HPD]: 24.5–38.1 Ma).

2.4. Ancestral range reconstruction

Ten geographic regions were defined based on paleogeographic and climatic evidence conforming to regions recognized in the World Geographical Scheme for Recording Plant Distributions (Brummitt, 2001). Geographic regions were defined as: A. Southern Africa; B. Tropical Africa (excluding Madagascar, the Mascarene, and the Seychelles Islands); C. Australia and Papua New Guinea (hereafter referred to as Australia); D. Asia; E. New Zealand and New Caledonia (hereafter referred to as New Zealand); F. Central and South America; G. North America and Mexico; H. Pacific Islands (including the Austral Islands, Fiji, Hawai'i, the Marquesas Islands, Samoa, the Society Islands, and Vanuatu); I. Western Indian Ocean Islands, (including Madagascar, the Mascarene, and the Seychelles Islands); and J. the Indian subcontinent. Each ingroup taxon was coded to one or more geographic areas according to its extant distribution, which was assessed based on searches of the literature (George, 1986, 1987; Wiland, 1997; Judd, 2000; Shu, 2000a; 2000b; Wiland-Szymańska, 2001; 2002; Pena et al., 2008; Singh, 2009; Manning and Goldblatt, 2012; Snijman, 2013; Kocyan and Wiland-Szymańska, 2016, 2017) and web-based resources.

Ancestral ranges were reconstructed using the R package 'Bio-GeoBEARS' (Matzke, 2013, 2014). The inferred ancestor at each node was constrained to span a maximum of three regions. The maximum clade credibility tree generated in BEAST was trimmed so that each species was represented by a single individual and to remove outgroup taxa. The maximum likelihood approximation (DIVALIKE) of the dispersal-vicariance method (DIVA) (Yu et al., 2010) and the dispersal-extinction-cladogenesis (DEC) (Ree and Smith, 2008) model, including and excluding a "j" parameter representing founder-event speciation, were applied. The biogeographic model (DIVALIKE or DEC) that represented the best fit to the data was selected using the cAIC. Statistical model selection methods were not applied for comparison of the model fit where a jump dispersal parameter "j" was included as this has recently been shown to be inappropriate (Ree and Sanmartin, 2018).

2.5. Diversification rates

We tested for shifts in diversification rates in the astelioid phylogeny in Bayesian Analysis of Macroevolutionary Mixtures (BAMM version 2.5.0) (Rabosky et al., 2014) including a sample fraction of species represented per family) (Table 4). The model priors were estimated using the "setBAMMpriors" function in the package 'BAMMTOOLS' version 2.1.7 in R with a conservative prior for the expected number of shifts set to one (Rabosky, 2014; Rabosky et al., 2017). We ran two analyses of one million generations using four chains. The first twenty-five percent of the trees generated during MCMC sampling were discarded as burn-in. Effective sampling size (ESS) values greater than 200 were achieved. Speciation and extinction rates through time and credible and best shift configurations were plotted and clade specific diversification rates were calculated.

3. Results

3.1. Phylogenetic analysis and tree topology

Summary statistics for the sequence data are provided in Table 1. Eight sections within the *trn*SG intergenic spacer (412 base pairs [bp]) were removed due to alignment ambiguities. The plastid dataset included 6586 bp of aligned sequence data. For MP, ML, and BA analyses, the tree topologies based on individual plastid DNA regions were broadly congruent; without conflicts among topologies for well supported nodes allowing individual markers to be concatenated for

phylogenetic reconstruction. Seven distinct partitions were recognized including the first, second, and third codon positions in *rbc*L and remaining markers were treated as distinct for parameter estimation.

The MP, ML, and BA analyses for the combined dataset resulted in similar tree topologies. The phylogeny generated in BA analyses is shown in Fig. 2. Lanariaceae and Hypoxidaceae were sister in all analyses (100 BP_P, 100 BP_{ML}, 1.00 PP) forming a sister clade to Asteliaceae (100 BP_P, 100 BP_{ML}, 1.00 PP). Blandfordiaceae was sister to Asteliaceae, Hypoxidaceae, and Lanariaceae clade (90 BP_P, 90 BP_{ML}, 1.00 PP) and Boryaceae was sister to the clade containing all other astelioid families (95 BP_P, - BP_{ML}, 0.84 PP).

Within the Asteliaceae (94 BP_P, 95 BP_{ML}, 1.00 PP), *Milligania* (95 BP_P, 86 BP_{ML}, 1.00 PP) was the sister clade to *Neoastelia* (100 BP_P, 100 BP_{ML}, 1.00 PP), and that clade was sister to the *Astelia* clade (100 BP_P, 100 BP_{ML}, 1.00 PP). Within Hypoxidaceae, three major clades were recovered: *Curculigo* + *Molineria* + *Hypoxidia* + *Neofriedmannia* ['A'; Fig. 2] (100 BP_P, 100 BP_{ML}, 1.00 PP) (hereafter called the *Curculigo* clade) and highlighting a taxonomic problem as *Curculigo* and *Molineria* species were mixed in two clades; *Pauridia* + *Empodium* ['B'; Fig. 2] (93 BP_P, 94 BP_{ML}, 1.00 PP) (hereafter called the *Pauridia* clade); and *Hypoxis* + *Rhodohypoxis* ['C'; Fig. 2] (100 BP_P, 100 BP_{ML}, 1.00 PP) (hereafter called the *Hypoxis* clade) with *Rhodohypoxis* deeply nested in *Hypoxis*. The interrelationship of the three main clades in the total evidence analysis remained unresolved. *Pauridia* (99 BP_P, 100 BP_{ML}, 1.00 PP) and *Empodium* (100 BP_P, 100 BP_{ML}, 1.00 PP) were each monophyletic. In maximum parsimony analyses, the *Curculigo* clade and the *Pauridia* clade were sister clades (78 BP_P) and that clade was the sister clade (100 BP_P) to the *Hypoxis* clade. Relationships within each of the Hypoxidaceae clades were broadly well resolved with support.

3.2. Divergence dating

The MRCA of the astelioid clade diverged in the Late Cretaceous at ca. 75.2 Ma (61.0–90.0 Ma) (Table 2; Fig. 3). The Hypoxidaceae + Lanariaceae + Asteliaceae clade diverged around the Paleocene to Eocene boundary at ca. 57.4 Ma (46.4–69.0 Ma) and the Hypoxidaceae + Lanariaceae clade shared a MRCA at ca. 50.5 Ma (40.3–61.4 Ma). Asteliaceae, Boryaceae, and Hypoxidaceae crown nodes are estimated to the Early Eocene (49.3 Ma; 37.1–61.7 Ma), Middle to Late Eocene boundary (37.8 Ma; 22.3–53.7 Ma), and Early Oligocene (32.5 Ma; 25.8–40.0 Ma), respectively. The crown age of Blandfordiaceae was estimated to ca. 3.2 Ma (1.4–5.2 Ma). ESS values for all estimated divergence dated nodes were >200.

3.3. Ancestral area reconstruction

The Dispersal Extinction Cladogenesis model was identified as the best-fit model (Table 3). Reconstructions and relative probabilities generated based on the DEC model, both with and without a "jump dispersal" parameter are provided in Table 2. Ancestral range reconstructions based on DEC and DEC + J models are largely consistent, with three exceptions, outlined below. Ranges reconstructed onto the phylogeny based on the DEC + J model are illustrated in Fig. 4.

The ancestral ranges of the Boryaceae and Blandfordiaceae crown nodes, were reconstructed as Australian (relative probabilities [rel. prob.] = 0.87 and 0.98, respectively). A southern African or Australian ancestral range was inferred for the crown Asteliaceae + Hypoxidaceae + Lanariaceae node based on the DEC (rel.prob. = 0.31) or DEC + J (rel. prob. = 0.45), respectively. An Australian ancestral range was inferred for the Asteliaceae crown node (rel. prob. = 0.66) and the *Milligania* + *Neoastelia* crown node (rel. prob. = 0.97). A New Zealand or Australian range was reconstructed for the *Astelia* crown node based on DEC (rel. prob. = 0.40) and DEC + J (rel. prob. = 0.39) reconstructions, respectively.

A southern African ancestral range was inferred for the MRCA of Hypoxidaceae + Lanariaceae (rel. prob. = 0.72), for the Hypoxidaceae
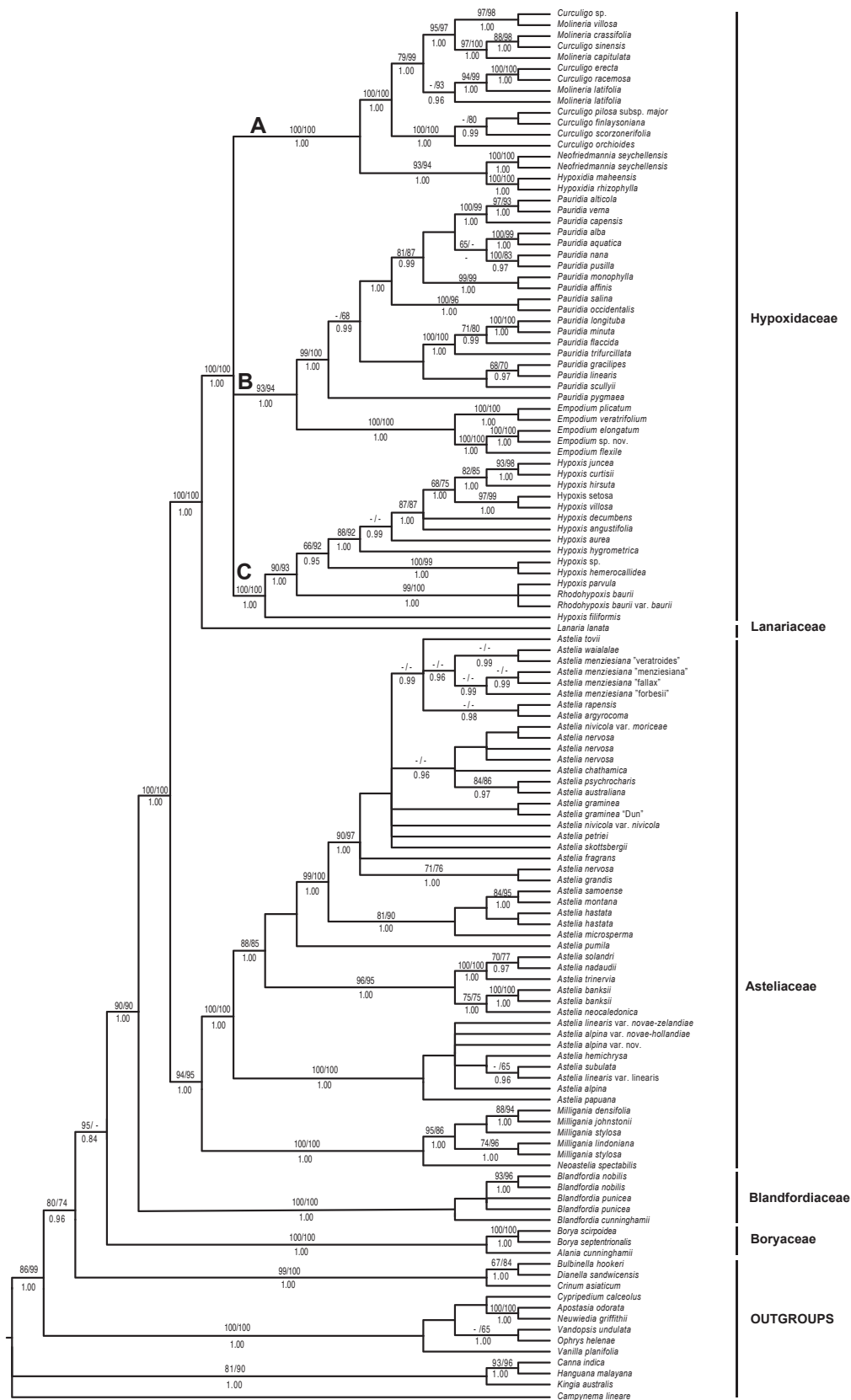
Fig. 2. Bayesian inference 50% consensus topology based on the concatenated dataset. Numbers above branches are bootstrap values (maximum parsimony/ maximum likelihood) and those below branches are Bayesian posterior probabilities. Bootstrap values >65% and posterior probabilities >0.90 are shown. Taxonomic treatment of *Pauridia* and *Astelia* is that of Snijman and Kocyan (2013) and Birch (2015), respectively.

Table 2
Divergence dates estimated using Bayesian inference in BEAST (Bouckaert et al., 2014). Constraints included a uniform distribution applied to the Asparagales crown node (121.32–111.32 million years) with date constraints drawn from Givnish et al. (2018); and (b) a prior of 26.0 million years applied to the *Astelia* crown node representing the earliest unequivocally determined *Astelia* fossil record (Birch and Keeley, 2013). Ancestral range reconstructions for the astelioid phylogeny using on the Dispersal Extinction Cladogenesis (DEC; Ree and Smith 2008) models with (DEC + J) and without a jump-dispersal parameter ("j") (DEC) as estimated in R package 'BioGeoBEARS' (Matzke, 2013, 2014). Na = Not applicable as monotypic family or genus.

Lineage	Date estimates (million years [Ma]; 95% Highest Posterior Density values) Crown group	Ancestral range (DEC model/ DEC + J model)	
		Range (Code)[+]	Probability
Astelioid clade (Asteliaceae + Blandfordiaceae + Boryaceae + Hypoxidaceae + Lanariaceae)	75.2 (61.0–90.0)	Australia	0.05/0.12
Asteliaceae + Blandfordiaceae + Hypoxidaceae + Lanariaceae	69.0 (55.6–82.6)	Australia	0.23/0.54
Asteliaceae + Hypoxidaceae + Lanariaceae	57.4 (46.4–69.0)	Southern Africa/Australia	0.31/0.45
Hypoxidaceae + Lanariaceae	50.5 (40.3–61.4)	Southern Africa	0.61/0.72
Asteliaceae	49.3 (37.1–61.7)	Australia	0.28/0.66
Blandfordiaceae	3.2 (1.4–5.2)	Australia	0.96/0.98
Boryaceae	37.8 (22.3–53.7)	Australia	0.66/0.87
Hypoxidaceae	32.5 (25.8–40.0)	Southern Africa	0.81/0.85
Lanariaceae	Na	Na	Na
Alania	Na	Na	Na
Astelia[*]	25.3 (24.1–27.1)	New Zealand/Australia	0.40/0.39
Blandfordia	3.2 (1.4–5.2)	Australia	0.96/0.98
Borya	0.4 (0.0–1.2)	Australia	1.00/1.00
Curculigo + Hypoxidia clade	16.9 (12.1–21.8)	Asia + Western Indian Ocean Islands/Western Indian Ocean Islands	0.19/0.26
Curculigo (excluding *Neofriedmannia seychellensis* + *Hypoxidia* clade)	13.2 (9.4–17.3)	Asia	0.38/0.55
Empodium	7.7 (4.4–11.3)	Southern Africa	0.96/0.98
Neofriedmannia	0.4 (0–1.2)	Na	Na
Hypoxidia	3.2 (1.2–5.6)	Western Indian Ocean Islands	0.98/0.99
Hypoxis clade	10.4 (7.1–14.0)	Southern Africa	0.82/0.82
Hypoxidia + *Neofriedmannia*	12.5 (7.7–17.6)	Western Indian Ocean Islands	0.80/0.88
Milligania	1.8 (0.7–3.1)	Australia	0.99/1.00
Neoastelia + Milligania	5.8 (2.9–9.2)	Australia	0.93/0.97
Neoastelia	Na	Na	Na
Pauridia	23.3 (18.3–28.7)	Southern Africa	0.97/0.98
Pauridia + Empodium	28.5 (22.5–34.9)	Southern Africa	0.96/0.97
Pauridia + Empodium + Curculigo	31.8 (25.2–39.1)	Southern Africa	0.84/0.86
Rhodohypoxis	Na	Na	Na

[*] Node with date constraint applied.

[+] Where a single ancestral range reconstruction is provided range reconstruction results based on DEC and DEC + J models are the same.

(rel. prob. = 0.85), *Empodium* (rel. prob. = 0.98), the *Hypoxis* clade (rel. prob. = 0.82), and *Pauridia* (rel. prob. = 0.98) crown nodes. The crown node of the *Curculigo* clade was reconstructed as occupying a widespread Asian + Western Indian Ocean Islands or Western Indian Ocean Islands

range based on DEC (rel. prob. = 0.19) and DEC + J (rel. prob. = 0.26) reconstructions, respectively. Within *Pauridia*, a single range expansion from Africa to Australia was inferred for the clade containing the Australian *Pauridia occidentalis* and *P. salina*. Of these ranges inferred for clades within *Hypoxis* only that inferring a North American range for the MRCA of *H. hirsuta* plus *H. juncea* plus *H. curtissii* received any (moderate) support.

3.4. Diversification rates

No net-diversification rate-shifts were identified within the astelioid clade with the highest posterior probability supporting a single rate across the clade. Net-diversification rate was highest for Hypoxidaceae ($r = 0.053$ per million years [Myr^{-1}]), followed by Asteliaceae ($r = 0.046$ Myr^{-1}), Blandfordiaceae ($r = 0.027$ Myr^{-1}), and Boryaceae ($r = 0.027$ Myr^{-1}) (Table 4). Mean mutation rates (μ) ranged from $\mu = 0.25$ extinctions Myr^{-1} to $\mu = 0.26$ extinctions Myr^{-1} for all astelioid families for which these data were calculated.

4. Discussion

4.1. Phylogenetic relationships

The first molecular phylogeny with comprehensive sampling of all currently accepted astelioid genera is presented. The monophyly of the astelioid clade is confirmed with – however – relatively low support values. Four major clades are identified representing the respective families in ascending order: Boryacae, Blandfordiaceae, Asteliaceae and Hypoxidaceae plus Lanariaceae – the latter being a monospecific family. This topology is consistent with results of other large-scale studies (Chen et al., 2013; Givnish et al., 2018). The low statistical support for the astelioid branch is probably an artifact of our limited sequence sampling as similar support values were detected in the four gene analyses by Chen et al. (2013) and in the four plastid gene analyses of Givnish et al. (2018) whereas in the 77 plastid gene analyses of Givnish et al. (2018) astelioid monophyly was unequivocal. All other nodes in the backbone of our tree receive almost maximal support and relationships are in concordance with other studies (Kocyan et al., 2011; Birch et al., 2012; Chen et al., 2013). The majority of generic clades represent taxonomic unity. *Astelia* (Birch, 2015) and *Pauridia* (Snijman and Kocyan, 2013) have recently been recircumscribed. *Hypoxis/Rhodohypoxis* is one of the exceptions and work is underway to unify them into *Hypoxis*. The situation in *Curculigo/ Molineria* is more difficult as discussed in Kocyan et al. (2011).

4.2. Molecular divergence dating

Astelioid families diversified after a recent pulse of monocotyledon diversification (50–60 Ma) that was recognised by Givnish et al. (2018). Crown Asteliaceae diversified from the Early to Middle Eocene boundary, contemporaneous with the diversification of crown Asparagaceae s.*l.* and crown Amaryllidaceae (ca. 49.5 Ma and ca. 46.8 Ma, respectively; Givnish et al., 2018). Crown Boryaceae and crown Hypoxidaceae diversified from the Middle to Late Eocene boundary and the Early Oligocene, respectively, contemporaneous with crown Asphodelaceae (ca. 42.2 Ma; Givnish et al., 2018). Our date estimates are older than those calculated by Chen et al. (2013) for astelioid families although our median dates fall within the ranges of their corresponding 95% HPD values. Our divergence date estimates are based on more comprehensive astelioid generic and species diversity and studies with more complete taxonomic sampling typically retrieve earlier date estimates (Linder et al., 2005).

4.3. Ancestral area reconstruction and diversification rate analyses

Early diverging astelioid lineages are reconstructed to Australia with diversification since ca. 75.2 Ma. At this time, Australia was part of a high-latitude Antarctic-Australasian landmass with a humid, ever-wet
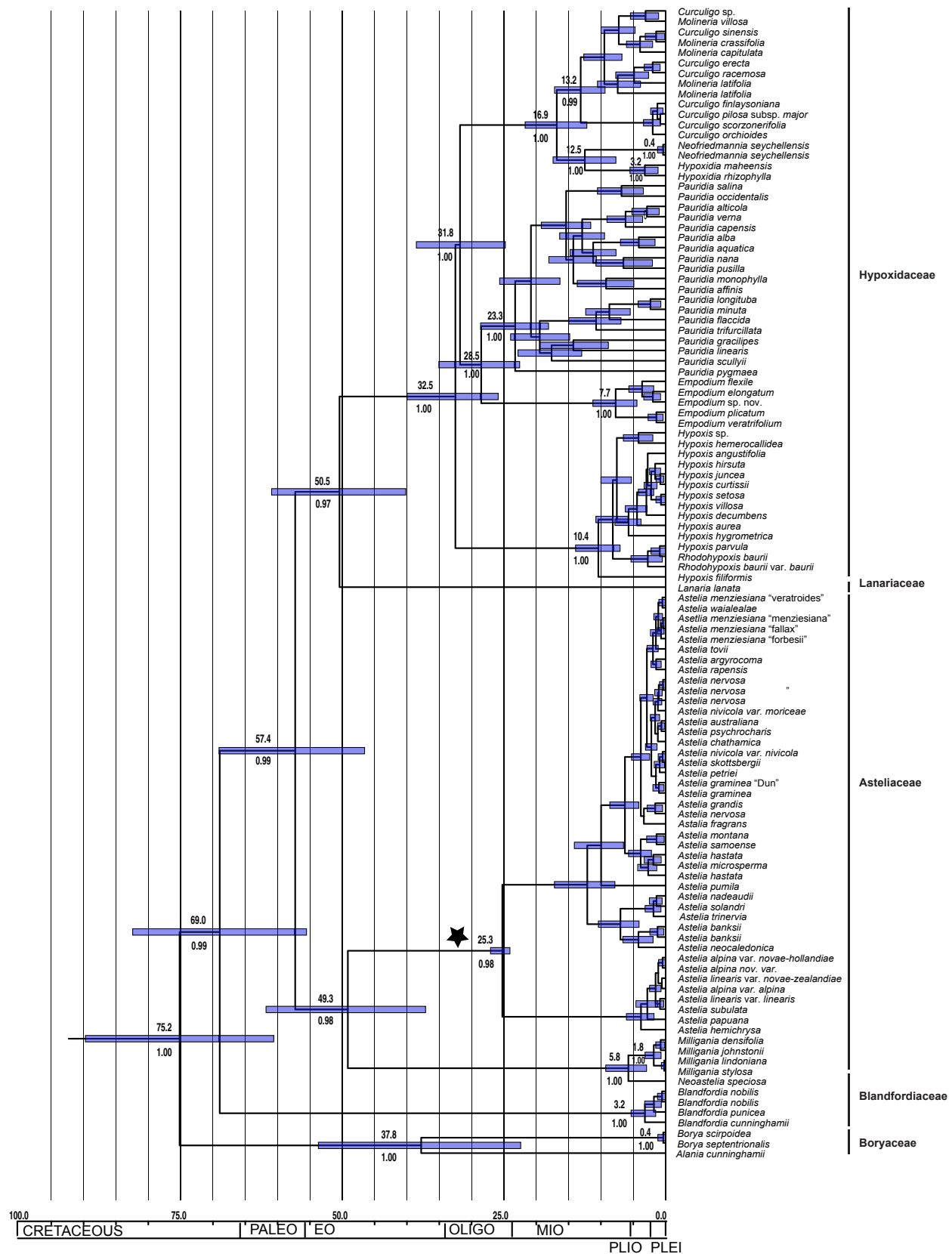
Fig. 3. Astelioid clade chronogram with divergence dates estimated using Bayesian inference conducted in BEAST (Bouckaert et al., 2014). Constraints included (a) a uniform distribution applied to the Asparagales crown node (121.32–111.32 million years) with date constraints drawn from Givnish et al. (2018); and (b) a prior (indicated by the star) of 26.0 million years applied to the *Astelia* crown node representing the earliest unequivocally determined *Astelia* fossil record (Birch and Keeley, 2013). Bars indicate 95% highest posterior density values. Geological time scale is shown at the bottom: Paleo = Palaeocene, Eo = Eocene, Oligo = Oligocene, Mio = Miocene, Plio = Pliocene, and Plei = Pleistocene. Geologic times are as per Berggren et al. (1995).

Table 3

Ancestral geographic range reconstruction parameters for Dispersal-Vicariance Analyses like (Ronquist, 1997) and Dispersal Extinction Cladogenesis (Ree and Smith, 2008) models with estimations completed in R package 'BioGeoBEARS' (Matzke, 2013, 2014). Na = statistical comparisons not conducted.

Models	Log likelihood (LnL)	Degrees of freedom (DF)	Rate of dispersal (D)	Rate of extinction (E)	Relative probability of founder-event speciation at cladogenesis (J)	Corrected Akaike information criterion (cAIC)
DIVALIKE	−222.8	2	0.0100	0.0100	0	449.7
DIVALIKE + J	Na	Na	0.0023	1.0×10^{-12}	0.0150	Na
DEC	−193.7	2	0.0110	0.2800	0	391.6
DEC + J	Na	Na	0.0039	0.0760	0.0140	Na

Table 4

Estimates of speciation (lambda), extinction (mu), and net diversification parameters per million years (Myr^{-1}) calculated for astelioid families estimated in BAMMtools (Rabosky et al., 2014). Mean ($\bar{x}$), 0.05, and 0.95 quantile values on the posterior distribution of rates at a given point in time are provided for speciation and extinction.

Family or clade	Sampling fraction	Lambda (λ) $\bar{x}$ (0.05, 0.95 quantiles)	Mu (μ) $\bar{x}$ (0.05, 0.95 quantiles)	Diversification (r) $\bar{x}$ (0.05, 0.95 quantiles)
Astelioid clade	96[a]/183	0.30 (0.22, 0.39)	0.25 (0.17, 0.36)	0.045
Asteliaceae	36/37	0.31 (0.23, 0.40)	0.26 (0.17, 0.36)	0.046
Blandfordiaceae	3/4	0.29 (0.21, 0.38)	0.26 (0.17, 0.36)	0.027
Boryaceae	3/12	0.29 (0.21, 0.38)	0.26 (0.21, 0.38)	0.027
Hypoxidaceae	53/130	0.31 (0.23, 0.40)	0.26 (0.16, 0.36)	0.053

[a] Astelioid clade includes the monotypic Lanariaceae, which was not separately parametised.

climate (Dingle and Lavelle, 2000) with subtropical rainforests over much of the Australian continent (Byrne et al., 2011). Despite the diverse species richness of astelioid families, no significant diversification shifts, either accelerations or decelerations, were identified for this lineage based on the markers sampled. Estimated extinction rates are uniform for astelioid families. The species rich families, Hypoxidaceae and Asteliaceae, have only slightly higher speciation rates. For astelioid families, differences in lineage specific speciation and extinction rates do not appear to be driving differences in species richness among families. Extrinsic factors such as habitat turnover and climatic change are influencing species diversity and will be discussed in a biogeographical context. Investigation of the influence of geographic area or habitat on net-diversification rates (see for example, the study of Gesneriaceae diversification [Roalson and Roberts, 2016]) warrants further study for astelioid genera, which differ in species richness and habitat diversity. That study would benefit from inclusion of additional sequence data, optimally sampling from multiple genomes, and increased sampling of *Hypoxis*, the most species-rich genus.

4.3.1. The astelioid clade in the context of Gondwanan biogeography

Our results suggest that extant astelioid family and generic speciation events have not been shaped by Gondwanan vicariance. Divergence of the African (Hypoxidaceae + Lanariaceae) and Australian (Asteliaceae) clades at ca. 57.4 Ma postdates the separation of Africa-Madagascar-India from East Gondwana (from ca. 162 Ma; McLoughlin, 2001). Divergence of Asteliaceae and Hypoxidaceae + Lanariaceae is therefore likely to be the result of long-distance dispersal across the proto Indian Ocean. At the Paleocene to Eocene boundary, distances between Australia-Antarctica and Africa-Madagascar were shorter than after this time period (Scotese et al., 1988). Allowing for founder-event speciation, the DEC + J model infers a single dispersal from Australia-Antarctica to Africa during the late Palaeocene. The reconstruction inferred based on the DEC model requires two range expansions, from Australia-Antarctica to Africa followed by a dispersal back to Australia, which is plausible, though a less compelling biogeographical scenario. Long-distance dispersal from Australasia to Africa has been proposed in Iridaceae: the ancestors of the sister clade to Australasian *Patersonia, Geosiris-Aristea-Nivenioideae-Crocoideae* likely reached Africa-Madagascar during the Early Eocene (Goldblatt et al., 2008). A westward dispersal from Australia via Antarctica-South American to Africa cannot be ruled out. However, we consider that pathway less likely as

astelioid diversity is depauperate in South America and no species from any of the early diverging lineages occur there.

An African ancestral range was inferred for the MRCA of the African stem *Pauridia* and Indian-Asian stem *Curculigo* clades. Their divergence during the Oligocene (ca. 31.8 Ma) postdates the tectonic rifting of West and East Gondwana, which separated Africa and Madagascar-Seychelles-India-Antarctica-Australia from ca. 113 to 132 Ma (McLoughlin, 2001). Therefore, transoceanic long distance-dispersal from Africa to the Seychelles or India-Asia is inferred. This divergence is concurrent with establishment of the circum-Antarctic current and the onset of Antarctic glaciation, which is thought to have driven cooling and aridification globally (Lewis et al., 2008). Overland dispersal pathways from Africa to Asia could have been mediated by stepping-stone dispersal via the African intermontane floristic corridor from the Oligocene onwards (Chorowicz, 2005; Givnish et al., 2016). Dispersal from Africa to Asia during a similar timeframe is also documented for *Cucumis* (Sebastian et al., 2010), *Gaertnera* (Malcomber, 2002), and *Gloriosum* (Givnish et al., 2016).

The presence of *Astelia* in South America and of *Curculigo* and *Hypoxis* in the New World is the result of multiple long-distance dispersal events, with dispersal inferred from New Zealand (*Astelia*), from Africa (*Hypoxis*), and from Asia (*Curculigo*). The relationships and timing of divergence of South American *Astelia pumila* remains unresolved. Either *A. pumila* is sister to an Australasian and Pacific clade with divergence in the Late Miocene (this study) or it is sister to a New Zealand, Pacific, and New Caledonian clade with divergence from the Oligocene (Birch et al., 2012). An earlier date would favour long-distance dispersal via Antarctic coastal forests (Birch et al., 2012), the later would require a transoceanic dispersal following elimination of coastal forest in Antarctica during the Miocene.

4.3.2. Variable species richness and extinction in the Asteliaceae

Crown Asteliaceae has an Australian ancestral range and radiated from the Early to Middle Eocene boundary (ca. 49.3 Ma) onwards. Long stem branches are observed for *Astelia* and *Milligania + Neoastelia* extending until the Late Oligocene (ca. 25.3 Ma) and Late Miocene (ca. 5.8 Ma), respectively. Pulses of diversification separated by long branches may indicate a history of extinction (see Crisp et al., 2011). Crown Asteliaceae nodes reconstructed as Australian (e.g. *Milligania, Neoastelia*) diversified from the Late Miocene onwards. All Australian taxa occur in mesic habitats, including wet rainforest (e.g. *N. spectabilis*)
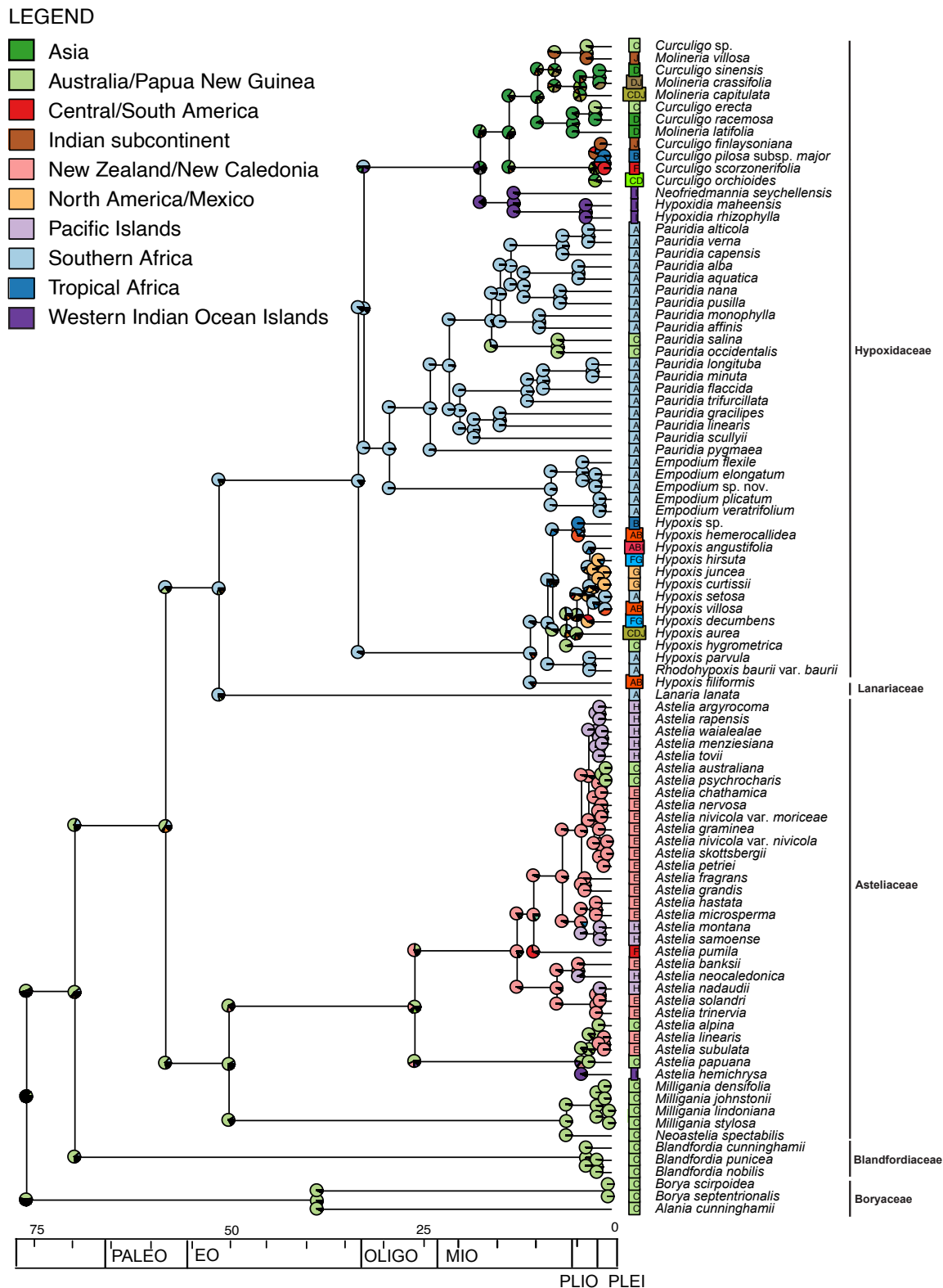
Fig. 4. Ancestral geographic ranges for the astelioid clade reconstructed onto the chronogram generated in BEAST (Bouckaert et al., 2014) using the Dispersal Extinction Cladogenesis (Ree and Smith, 2008) models with a "j" parameter allowing for founder event speciation estimated in BioGeoBEARS (Matzke, 2013, 2014). Geological time scale is shown at the bottom: Paleo = Palaeocene, Eo = Eocene, Oligo = Oligocene, Mio = Miocene, Plio = Pliocene, and Plei = Pleistocene. Geologic times are as per Berggren et al. (1995). Geographic regions were defined as: A. Southern Africa; B. Tropical Africa, excluding Madagascar, the Mascarene, and the Seychelles Islands; C. Australia and Papua New Guinea; D. Asia; E. New Zealand and New Caledonia; F. Central and South and America; G. North America and Mexico; H. Pacific Islands, including the Austral Islands, Fiji, Hawai'i, the Marquesas Islands, Samoa, the Society Islands, and Vanuatu; I. Western Indian Ocean Island, including Madagascar, the Mascarene, and the Seychelles Islands; and J. the Indian subcontinent.

and alpine herbfields (e.g. *A. alpina, M. lindoniana*). In Australia, mesic habitat contracted during the Late Miocene and Pliocene (Byrne et al., 2011) associated with reduction in rainfall and increasing rainfall seasonality (Hill, 2004), which may have caused extinctions in this lineage. Low species richness of *Milligania* and *Neoastelia* may reflect an inability of those lineages to undergo range shifts to continuously occupy mesic habitats or to adapt, as necessary, to enable occupancy of drier habitats.

Crown *Astelia* diversified since the Late Oligocene (ca. 25.3 Ma), with an ancestral range inferred as either Australia (DEC + J model) or New Zealand (DEC model). *Astelia s.l.* is documented in the New Zealand fossil record, represented by microfossils dated to the Middle Oligocene (Couper, 1960) and pollen and leaf cuticle fossils from the Early Miocene (Mildenhall and Pocknall, 1989; Pole, 2007; Maciunas et al., 2011). *Astelia* is recorded in the Australian fossil record from the Late Pliocene (MacPhail et al., 1993) or the Quaternary (MacPhail et al., 1994). For all models investigated (DIVA, DIVA + J, DEC) except that based on DEC + J, the crown *Astelia* range reconstruction includes New Zealand. A widespread range spanning New Zealand and Australia was also inferred for crown *Astelia* in a biogeographic analyses applying the DEC model for ancestral area reconstructions (using an Asteliaceae phylogeny inferred from chloroplast and nuclear data) (Birch and Keeley, 2013). The ancestral range of crown *Astelia* is equivocal based on current analyses. But, fossil data clearly indicate occupancy of *Astelia* in New Zealand early in the evolutionary history of the genus. Resolution of *Astelia*, species relationships, particularly within *Astelia* subg. *Astelia*, which includes species from Australia, Papua New Guinea, and New Zealand may enable unequivocal determination of the crown *Astelia* ancestral range.

Subsequent diversification of *Astelia* in New Zealand only occurred from the Middle Miocene (ca. 12.1 Ma) onwards. During the Oligocene New Zealand was approximately 20% of its present size (Lee et al., 2001) and loss of terrestrial habitat during that time may have resulted in extinctions in many lineages. The New Zealand landmass expanded to its present size by the Late Miocene (Lee et al., 2001) and during the Pliocene–Pleistocene extensive uplift generated high altitudes and alpine habitat (Lee et al., 2001). This coincides with a fairly rapid diversification into mesic and alpine habitats, to which *Astelia* may have been pre-adapted, if the occupancy of wet habitats with periodically inundated soils by many extant taxa is indicative of ancestral ecological tolerances.

4.3.3. Africa as a secondary center of diversity in astelioids

Our biogeographical results establish a timeframe for diversification of the Hypoxidaceae and Lanariaceae lineage for the first time. Lanariaceae is one of 28 plant monotypic families world-wide (Christenhusz and Byng, 2016). As it is monotypic, we are only able to estimate the timing of divergence from the MRCA shared with Hypoxidaceae. We cannot say with certainty whether this lineage has always been monospecific or if this is the result of possible extinction events. Lanariaceae occurs solely in the Cape region of South Africa where it is an element of fynbos vegetation. However, it is unlikely that Lanariaceae evolved in the same type of vegetation, as during the Early Eocene the climate was much warmer than today and the Cape region was still forested.

Southern Africa is inferred as the ancestral area for Hypoxidaceae. While the relationships of the three main Hypoxidaceae clades remain equivocal we consider it unlikely that the African origin inferred for Hypoxidaceae will alter with increased sampling or once relationships of those clades are resolved. All the basal lineages in the three main Hypoxidaceae clades occur in Africa or the floristically strongly related Seychelles – and the Lanariaceae is only known from South Africa. The Hypoxidaceae experienced a pulse of diversification during the Early Oligocene, including divergence of stem *Hypoxis* (ca. 32.5 Ma), stem *Curculigo* (ca. 31.8 Ma), and stem *Pauridia* (ca. 28.5 Ma). This pulse of diversification coincides with the establishment of the circum-Antarctic current and the onset of Antarctic glaciation (Lewis et al., 2008). Divergence of the Hypoxidaceae from 32.5 Ma is temporally coincident

with radiation of other African Austro-temperate lineages (e.g. African Restionaceae) during the Eocene (Galley and Linder, 2006; Linder, 2014).

Crown *Pauridia* has undergone steady diversification from the Late Oligocene to Early Miocene boundary (ca. 23.3 Ma). In the early Miocene woodland-savanna vegetation was present in southern African interior plateau and summer wet conditions supported subtropical rainforest in the southern coastal lowlands (Linder, 2003; van Zinderen Bakker and Mercer, 1986). Extant *Pauridia* are almost all endemic to the Cape Floristic Province where they occupy damp habitats within fynbos and renosterveld vegetation (Mucina and Rutherford, 2006). *Pauridia* likely persisted in damp habitats and diversified throughout the increasingly arid and seasonal conditions that developed in southern Africa during the Late Miocene to Early Pliocene (Coetzee, 1983; van Zinderen Bakker and Mercer, 1986; Verboom et al., 2014).

Conversely, *Hypoxis* and *Empodium* have radiated only since the Late Miocene (ca. 10.4 Ma and 7.7 Ma, respectively). Diversification of these genera coincides with the development of seasonality, of cooling, and increasing aridity in the southern African flora, which is generally thought to have been initiated during the Late Miocene (ca. 10 Ma) as a result of the establishment of the Benguela Upwelling System and has intensified since that time (van Zinderen Bakker and Mercer, 1986). Early diversification of *Hypoxis* predated coastal uplift that occurred from the late Pliocene onward, which generated the plateau-escarpment, narrow-coastal-belt landscape of contemporary southern Africa (Goldblatt, 1978). The intensification of aridification from the mid-Pliocene cooling onwards and the resulting opening up of closed forests and woodlands into savanna and grasslands (van Zinderen Bakker and Mercer, 1986) would have expanded availability of habitat for *Hypoxis*, which occurs primarily in the grassland biome (Singh, 2009). The rapid diversification of *Hypoxis* in Africa may have been possible due, in part, to expansion of these grassland habitats, which would have initially provided open niches for colonization.

The absence of evident cladogenesis on the stem Hypoxidaceae during the Late Eocene and Early Oligocene may indicate lack of diversification, potentially as a result of stable climatic conditions and high niche occupancy during the Eocene. The long stem *Hypoxis* and *Empodium* branch lengths may also indicate an extinction history during the Early Miocene. However, estimation of Hypoxidaceae radiation rates awaits more comprehensive sampling of African *Hypoxis*. Specifically, more comprehensive sampling of central and northern African *Hypoxis* taxa is necessary to understand the biogeographical relationships and estimate diversification times of tropical African *Hypoxis*, which are represented in this study only by *H. angustifolia*.

In Hypoxidaceae, two Pliocene African and American disjunctions are inferred; that of African (*Hypoxis setosa*, *H. villosa*) and American (*H. curtissii*, *H. hirsuta*, *H. juncea*) clades (ca. 2.5 Ma) and that of African *Curculigo pilosa* and American *C. scorzonerifolia* (ca. 2.2 Ma). These recent splits are well after the formation of the Atlantic Ocean, which opened from ca. 135 to 105 Ma (McLoughlin, 2001). Late Miocene (ca. 6.8 Ma) transoceanic long-distance dispersals from Africa to Australia are also inferred to account for extant Australian *Pauridia occidentalis* and *P. salina*, which are nested within an otherwise African clade and for *Hypoxis*, with divergence of Australian *H. hygrometrica* from its sister clade (ca. 5.7 Ma). This is consistent with a pattern of Neogene exchange between the African Cape and Australian floras, which has frequently occurred from Africa to Australia (Linder, 2014).

4.3.4. An Asian diversification of Curculigo and Molineria from the Middle Miocene

Ancestral range reconstructions infer close connections between the Africa and Asian floras in the *Curculigo* clade (including *Molineria*, *Hypoxidia*, and *Neofriedmannia*). A southern African range was reconstructed for stem *Curculigo* clade. However, the ancestral range of the crown *Curculigo* clade remains equivocal, with models inferring either a widespread distribution spanning Western Indian Ocean Islands and

Asia and subsequent subdivision of that ancestral range (DEC) or a narrow range on Western Indian Ocean Islands and subsequent clado-genetic dispersal to Asia (DEC + J). These reconstructions place ancestral nodes of the *Curculigo* clade in Asia, at least from 13.2 Ma (crown *Curculigo* + *Molineria* clade, as reconstructed based on the DEC + J model) or earlier from 16.9 Ma (crown *Curculigo* clade, as reconstructed based on the DEC model).

The Middle Miocene divergence of the MRCA of the *Curculigo* + *Molineria* clade (13.2 Ma) places that diversification soon after the Middle Miocene Climatic Optimum (ca. 15–18 Ma). Within the *Curculigo* + *Molineria* clade, three clades are recovered. In two of these clades, taxa that are currently widespread throughout Asia are sister to clades containing taxa with narrower geographic ranges. A clade containing the widespread Southeast Asian (Indonesia, Malaysia, Philippines) *Molineria latifolia* is sister to a Papua New Guinea and Borneo clade and divergence of the MRCA of the Southeast Asian and Papua New Guinea plus Borneo clades occurred from the Early Pliocene, after uplift in New Guinea, which occurred from the Middle to Late Miocene (Morley, 2003). In Australia, *Curculigo* can be considered a tropical element with recent origins from Southeast Asia (Nelson and Platnick, 1981) as is seen for multiple Australian lowland tropical rainforest lineages (Sniderman and Jordan, 2011). Northern Chinese endemic taxa (*C. sinensis*, *M. crassifolia*) occur in high elevation habitats. Their divergence from widespread Southeast Asian *Molineria capitulata* during the Early Pliocene is after a period of rapid uplift that would have expanded high elevation habitat within the Tibetan Plateau during the late Miocene and Pliocene (Li et al., 2014). The clade in which the widespread Asian species *C. orchioides* is sister to a clade containing Indian (*C. finlaysoniana*), South American (*C. scorzonerifolia*), and African (*Curculigo pilosa*) species has radiated only since the Late Pliocene. The recent diversification of this clade combined with species distributions spanning continents indicates extensive biotic exchange, which could potentially have involved both overland (among Asia, India, and Africa) and/or transoceanic (between Asia and Africa) dispersal pathways, but also dispersal by humans may not be excluded (Kocyan et al., 2011).

5. Conclusions

Our analyses imply a Late Cretaceous (around 75 Ma) rise of the astelioid clade. This implies that – other than suggested by current distribution – astelioids do not have a Gondwanan origin. Rather, the MRCA of the Astelioid clade originated on the Antarctic-Australasian landmass. The current distribution of the two main clades – Asteliaceae and Hypoxidaceae – with Australian-New Zealand and African origins – implies that astelioids have reached their current distribution via various long-distance dispersal events. The data investigated here imply that *Hypoxis* diversified in Africa with the expansion of grassland habitat during the Late Miocene and that of *Astelia* in New Zealand with the expansion of alpine habitat during the Pliocene.

Though our study represents the most comprehensively sampled study of the astelioid clade at the generic rank, it has its limitations due to inclusion of a small number of genetic markers; an NGS approach using genetic markers of multiple genomes would hold potential to generate sufficient variation to clarify Hypoxidaceae relationships and those within *Astelia*. Further astelioid research is warranted with much-extended sampling within the Hypoxidaceae, particularly of *Hypoxis*, to fully understand the biogeographic history of the family.

Data availability

DNA sequences: GenBank accession numbers are provided in Appendix 1.

CRediT authorship contribution statement

Joanne L. Birch: Conceptualization, Methodology, Formal analysis,

Investigation, Data curation, Validation, Writing - original draft, Visualization, Funding acquisition. **Alexander Kocyan:** Conceptualization, Methodology, Formal analysis, Investigation, Data curation, Writing - review & editing, Funding acquisition.

Declaration of Competing Interest

The authors declare that they have no known competing financial interests or personal relationships that could have appeared to influence the work reported in this paper.

Appendix A. Supplementary data

Supplementary data to this article can be found online at https://doi.org/10.1016/j.ympev.2021.107203.

References

Bell, C.D., Soltis, D.E., Soltis, P.S., 2010. The age and diversification of the angiosperms re-visited. Am. J. Bot. 97, 1296–1303.

Berggren, W.A., Kent, D.V., Swisher, C.C., Aubry, M.-P., 1995. A revised Cenozoic geochronology and chronostratigraphy. In: Berggren, W.A., Kent, D.V., Aubry, M.-P., Hardenbol, J. (Eds.), Geochronology, Time Scales and Global Stratigraphic Correlation. SEPM Special Publication, Tulsa, Oklahoma, pp. 129–212.

Birch, J.L., 2015. A revision of infrageneric classification in *Astelia* Banks & Sol. ex. R.Br. (Asteliaceae). PhytoKeys 52, 105–132.

Birch, J.L., Keeley, S.C., 2013. Dispersal pathways across the Pacific: the historical biogeography of *Astelia s.l.* (Asteliaceae, Asparagales). J. Biogeogr. 40, 1914–1927.

Birch, J.L., Keeley, S.C., Morden, C.W., 2012. Molecular phylogeny and dating of Asteliaceae (Asparagales): *Astelia s.l.* evolution provides insight into the Oligocene history of New Zealand. Mol. Phylogen. Evol. 65, 102–115.

Bouchenak-Khelladi, Y., Verboom, G.A., Savolainen, V., Hodkinson, T.R., 2010. Biogeography of the grasses (Poaceae): a phylogenetic approach to reveal evolutionary history in geographical space and geological time. Bot. J. Linn. Soc. 162, 543–557.

Bouckaert, R., Heled, J., Kuhnert, D., Vaughan, T., Wu, C.-H., Xie, D., Succhard, M.A., Rambaut, A., Drummond, A.J., 2014. BEAST 2: A software platform for Bayesian evolutionary analysis. PLoS Comput. Biol. 10 (4), e1003537.

Bremer, K., Janssen, T., 2006. Gondwanan origin of major monocot groups inferred from dispersal-vicariance analysis. In: Columbus, J.T., Friar, E.A., Porter, J.M., Prince, L. M., Simpson, M.G. (Eds.), Monocots: Comparative Biology and Evolution (excluding Poales). Rancho Santa Ana Botanic Garden, Claremont, California, pp. 22–27.

Brummitt, R.K., 2001. World geographical scheme for recording plant distributions. Hunt Inst. for Botanical Documentation, Pittsburgh.

Byrne, M., Steane, D.A., Joseph, L., Yeates, D.K., Jordan, G.J., Crayn, D., Aplin, K., Cantrill, D.J., Cook, L.G., Crisp, M.D., Keogh, J.S., Melville, J., Moritz, C., Porch, N., Sniderman, J.M.K., Sunnucks, P., Weston, P.H., 2011. Decline of a biome: evolution, contraction, fragmentation, extinction and invasion of the Australian mesic zone biota. J. Biogeogr. 38, 1635–1656.

Carpenter, R.J., Macphail, M.K., Jordan, G.J., Hill, R.S., 2015. Fossil evidence for open, Proteaceae-dominated heathlands and fire in the Late Cretaceous of Australia. Am. J. Bot. 102, 2090–2107.

Chen, S., Kim, D.K., Chase, M.W., Kim, J.H., 2013. Networks in a large-scale phylogenetic analysis: reconstructing evolutionary history of Asparagales (Lilianae) based on four plastid genes. PLoS ONE 8, 1–18.

Chorowicz, J., 2005. The East African rift system. J. Afr. Earth Sci. 43, 379–410.

Christenhusz, M.J.M., Byng, J.W., 2016. The number of known plants species in the world and its annual increase. Phytotaxa 261, 201–217.

Coetzee, J.A., 1983. Intimations on the Tertiary vegetation of southern Africa. Bothalia 14, 345–354.

Couper, R.A., 1960. New Zealand Mesozoic and Cainozoic plant microfossils. Paleontological Bulletin 32. New Zealand Geological Survey, Wellington, New Zealand.

Crisp, M.D., Cook, L.G., Steane, D.A., 2004. Radiation of the Australian flora: what can comparisons of molecular phylogenies across multiple taxa tell us about the evolution of diversity in present-day communities. Philos. Trans. R. Soc. B 359, 1551–1571.

Crisp, M.D., Trewick, S.A., Cook, L.G., 2011. Hypothesis testing in biogeography. Trends Ecol. Evol. 26, 66–72.

Dingle, R.V., Lavelle, M., 2000. Antarctic peninsula late cretaceous-early Cenozoic palaeoenvironments and Gondwana palaeogeographies. J. Afr. Earth Sci. 31, 91–105.

Galley, C., Linder, H.P., 2006. Geographical affinities of the Cape flora, South Africa. J. Biogeogr. 33, 236–250.

George, A.S., 1986. Flora of Australia Volume 46 Iridaceae to Dioscoreaceae. Australian Government Publishing Service, Canberra ACT, Australia.

George, A.S., 1987. Flora of Australia Volume 45 Hydatellaceae to Liliaceae. Australian Government Publishing Service, Canberra ACT, Australia.

Givnish, T.J., Juluaga, A., Marques, I., Lam, V.K.Y., Gomez, M.S., Iles, W.J.D., Ames, M., Spalink, D., Moeller, J.R., Briggs, B.G., Lyon, S.P., Stevenson, D.W., Zomlefer, W., Graham, S.W., 2016. Phylogenomics and historical biogeography of the monocot order Liliales: out of Australia and through Antarctica. Cladistics 32, 580–605.

Givnish, T.J., Pires, J.C., Graham, S.W., McPherson, M.A., Prince, L.M., Patterson, T.B., Hardeep, S.R., Roalson, E.H., Evans, T.M., Hahn, W.J., Miliam, K.C., Meerow, A.W., Molvray, M., Kores, P., O'Brian, H.E., Hall, J.C., Kress, W.J., Sytsma, K.J., 2006. Phylogenetic relationships of monocots based on the highly informative plastid gene *ndh*F: evidence for widespread concerted convergence. Aliso 22, 28–51.

Givnish, T.J., Zuluaga, A., Spalink, D., Soto Gomez, M., Lam, V.K.Y., Saarela, J.M., Sass, C., Iles, W.J.D., de Sousa, D.J.L., Leebens-Mack, J., Pires, J.C., Zomlefer, W.B., Gandolfo, M.A., Davis, J.I., Stevenson, D.W., dePamphilis, C., Specht, C.D., Graham, S.W., Barrett, C.F., Ané, C., 2018. Monocot plastid phylogenomics, timeline, net rates of species diversification, the power of multi-gene analyses, and a functional model for the origin of monocots. Am. J. Bot. 105, 1888–1910.

Goldblatt, P., 1978. An Analysis of the flora of southern Africa: its characteristics, relationships, and origins. Ann. Missouri Bot. Gard. 65, 469–1436.

Goldblatt, P., Rodriguez, A., Powell, M.P., Davies, T.J., Manning, J.C., 2008. Iridaceae "out of Australasia"? Phylogeny, biogeography, and divergence time based on plastid DNA sequences. Syst. Bot. 33, 495–508.

Guindon, S., Gascuel, O., 2003. A simple, fast and accurate method to estimate large phylogenies by maximum-likelihood. Syst. Biol. 52, 696–704.

Gunn, B.F., Murphy, D.J., Walsh, N.G., Conran, J.G., Pires, J.C., Macfarlane, T.D., Birch, J.L., 2020. Evolution of Lomandroideae: multiple origins of polyploidy and biome occupancy in Australia. Mol. Phylogen. Evol. 149, 106836.

Hill, R.S., 2004. Origins of the southeastern Australian vegetation. Philos. Trans. R. Soc. B 359, 1537–1549.

Holdgate, G.R., Wallace, M.W., Gallagher, S.J., Wagstaff, B.E., Moore, D., 2008. No mountains to snow on: major post-Eocene uplift of the east Victoria highlands; evidence from Cenozoic deposits. Aust. J. Earth Sci. 55, 211–234.

Iles, W.J.D., Smith, S.Y., Gandolfo, M.A., Graham, S.W., 2015. Monocot fossils suitable for molecular dating analyses. Bot. J. Linn. Soc. 178, 346–374.

Judd, W.S., 2000. The Hypoxidaceae in the southeastern United States. Harv. Pap. Bot. 5, 79–98.

Kocyan, A., Snijman, D.A., Forest, F., Devey, D.S., Freudenstein, J.V., Wiland-Szymańska, J., Chase, M.W., Rudall, P.J., 2011. Molecular phylogenetics of Hypoxidaceae - evidence from plastid DNA data and inferences on morphology and biogeography. Mol. Phylogen. Evol. 60, 122–136.

Kocyan, A., Wiland-Szymańska, J., 2016. *Friedmannia*: a new genus from the Seychelles and the beginning of a generic realignment of *Curculigo* (Hypoxidaceae). Phytotaxa 283, 54–64.

Kocyan, A., Wiland-Szymańska, J., 2017. A new name and a new combination for *Friedmannia* nom. Illeg. (Hypoxidaceae). Phytotaxa 291, 239.

Lanfear, R., Frandsen, P.B., Wright, A.M., Senfeld, T., Calcott, B., 2016. PartitionFinder2: new methods for selecting partitioned models of evolution for molecular and morphological phylogenetic analyses. Mol. Biol. Evol. 34, 772–773.

Lee, D.E., Lee, W.G., Mortimer, N., 2001. Where and why have all the flowers gone? Depletion and turnover in the New Zealand Cenozoic angiosperm flora in relation to palaeogeography and climate. Aust. J. Bot. 49, 341–356.

Lewis, A.R., Marchant, D.R., Ashworth, A.C., Hedenäs, L., Hemming, S.R., Johnson, J.V., Leng, M.J., Machlus, L.M., Newton, A.E., Raine, J.I., Willenbring, J.K., Williams, M., Wolfe, A.P., 2008. Mid-Miocene cooling and the extinction of tundra in continental Antarctica. Proc. Natl. Aca. Sci. U.S.A. 105, 10676–10680.

Li, J., Fang, X., Song, C., Pan, B., Ma, Y., Yan, M., 2014. Late Miocene-Quaternary rapid stepwise uplift of the NE Tibetan Plateau and its effects on climatic and environmental changes. Quat. Res. 81, 400–423.

Linder, H.P., 2003. The radiation of the Cape flora, southern Africa. Biol. Rev. 78, 597–638.

Linder, H.P., 2014. The evolution of African plant diversity. Front. Ecol. Evol. 2, 38. https://doi.org/10.3389/fevo.2014.00038.

Linder, H.P., Eldenäs, P., Briggs, B.G., 2003. Contrasting patterns of radiation in African and Australian Restionaceae. Evolution 57, 2688–2702.

Linder, H.P., Hardy, C.R., Rutschmann, F., 2005. Taxon sampling effects in molecular clock dating: an example from the African Restionaceae. Mol. Phylogen. Evol. 35, 569–582.

Maciunas, E., Conran, J.G., Bannister, J.M., Paull, R., Lee, D.E., 2011. Miocene Astelia (Asparagales: Asteliaceae) macrofossils from southern New Zealand. Aust. Syst. Bot. 24, 19–31.

MacPhail, M.K., Alley, N.F., Truswell, E.M., Sluiter, I.R.K., 1994. Early Tertiary vegetation: evidence from spores and pollen. In: Hill, R.S. (Ed.), History of the Australian Vegetation: Cretaceous to Recent. Cambridge University Press, Cambridge, pp. 182–262.

MacPhail, M.K., Jordan, G.J., Hill, R.S., 1993. Key periods in the evolution of the flora and vegetation in western Tasmania I. the Early-Middle Pleistocene. Aust. J. Bot. 41, 673–707.

Malcomber, S.T., 2002. Phylogeny of *Gaertnera* Lam. (Rubiaceae) based on multiple DNA markers: evidence of a rapid radiation in a widespread, morphologically diverse genus. Evolution 56, 42–57.

Manning, J., Goldblatt, P., 2012. Plants of the Greater Cape Floristic Region 1: the Core Cape flora, Strelitzia 29. South African National Biodiversity Institute, Pretoria.

Matzke, M.J., 2013. Probabilistic historical biogeography; new models for founder-event speciation, imperfect detection, and fossils allow improved accuracy and model-testing. Front. Biogeogr. 5, 242–248.

Matzke, M.J., 2014. Model selection in historical biogeography reveals that founder-event speciation is a crucial process in island clades. Syst. Biol. 63, 951–970.

McLoughlin, S., 2001. The breakup history of Gondwana and its impact on pre-Cenozoic floristic provincialism. Aust. J. Bot. 49, 271–300.

Mildenhall, D.C., Pocknall, D.T., 1989. Miocene-Pleistocene spores and pollen from Central Otago, South Island, New Zealand. New Zealand Geological Survey Paleontological Bulletin 59. New Zealand Geological Survey, Auckland.

Morley, R.J., 2003. Interplate dispersal paths for megathermal angiosperms. Perspect. Plant Ecol. 6, 5–20.

Mucina, L., Rutherford, M.C., 2006. The Vegetation of South Africa, Lesotho and Swaziland. Strelitzia 19. South African National Biodiversity Institute, Pretoria.

Nelson, G., Platnick, N., 1981. Systematics and Biogeography. Columbia University Press, New York, NY.

Pena, M., Watanabe, M.T.C., Sano, P., 2008. Flora da Serra do Cipó, Minas Gerais: Hypoxidaceae. Bol. Bot. Univ. São Paulo 26, 161–164.

Pires, J.C., Maureira, I.J., Givnish, T.J., Sytsma, K.J., Seberg, O., Petersen, G., Davis, J.I., Stevenson, D.W., Rudall, P.J., Fay, M.F., Chase, M.W., 2006. Phylogeny, genome size, and chromosome evolution of Asparagales. Aliso 22, 287–304.

Pole, M., 2007. Monocot macrofossils from the Miocene of southern New Zealand. Palaeontol. Electron. 10, 15A.

Posada, D., 2008. JModelTest: phylogenetic model averaging. Mol. Biol. Evol. 25, 1253–1256.

Rabosky, D.L., 2014. Automatic detection of key innovations, rate shifts, and diversity-dependence on phylogenetic trees. PLoS ONE 9, e89543.

Rabosky, D.L., Grundler, M.C., Anderson, C.J., Title, P., Shi, J.J., Brown, J.W., Huang, H., Larson, J.G., 2014. BAMMtools: an R package for the analysis of evolutionary dynamics on phylogenetic trees. Methods Ecol. Evol. 5, 701–707.

Rabosky, D.L., Mitchell, J.S., Chang, J., 2017. Is BAMM flawed? Theoretical and practical concerns in the analysis of multi-rate diversification models. Syst. Biol 66, 477–498.

Rambaut, A., Drummond, A.J.. Tracer v1.5 [computer program]. Website. http://beast. bio.edu.ac.uk/Tracer.

Raven, P.H., Axelrod, D.I., 1974. Angiosperm biogeography and past continental movements. Ann. Missouri Bot. Gard. 61, 539–673.

Ree, R.H., Sanmartin, I., 2018. Conceptual and statistical problems with the DEC+J model of founder-event speciation and its comparison with DEC via model selection. J. Biogeogr. 45, 741–749.

Ree, R.H., Smith, S.Y., 2008. Maximum likelihood inference of geographic range evolution by dispersal, local extinction, and cladogenesis. Syst. Biol. 57, 4–14.

Revell, L.J., 2012. Phytools: An R package for phylogenetic comparative biology (and other things). Methods Ecol. Evol. 3, 217–223.

Roalson, E.H., Roberts, W.R., 2016. Distinct processes drive diversification in different clades of Gesneriaceae. Syst. Biol. 65, 662–684.

Ronquist, F., 1997. Dispersal-vicariance analysis: a new approach to the quantification of historical biogeography. Syst. Biol. 46, 195–203.

Ronquist, F., Teslenko, M., van der Mark, P., Ayres, D.L., Darling, A., Höhna, S., Larget, B., Liu, L., Suchard, M.A., Huelsenbeck, J.P., 2012. MRBAYES 3.2: Efficient Bayesian phylogenetic inference and model choice across a large model space. Syst. Biol. 61, 539–542.

RStudio, 2016. RStudio: integrated development for R. RStudio, Inc., Boston, MA. http://www.rstudio.com/.

Schliep, K.P., 2011. Phangorn: phylogenetic analysis in R. Bioinformatics 27, 592–593.

Scotese, C.R., Gahagan, L.M., Larson, R.L., 1988. Plate tectonic reconstructions of the Cretaceous and Cenozoic ocean basins. Tectonophysics 155, 27–48.

Sebastian, P., Schaefer, H., Telford, I.R.H., Renner, S.S., 2010. Cucumber (*Cucumis sativus*) and melon (*C. melo*) have numerous wild relatives in Asia and Australia, and the sister species of melon is from Australia. Proc. Natl. Aca. Sci. U.S.A. 107, 14269–14273.

Seberg, O., Petersen, G., Davis, J.I., Pires, J.C., Stevenson, D.W., Chase, M.W., Fay, M.F., Devey, D.S., Jorgensen, T., Sytsma, K.J., Pillon, Y., 2012. Phylogeny of the Asparagales based on three plastid and two mitochondrial genes. Am. J. Bot. 99, 875–889.

Singh, Y., 2009. Systematics of Hypoxis (Hypoxidaceae) in southern Africa. PhD Dissertation. University of Pretoria.

Shu, X.J.M.C., 2000a. Hypoxis. In: Wu, Z.Y., Raven, P.H. (Eds.), Flora of China 24. Science Press and Missouri Botanical Garden Press, Beijing and St. Louis, p. 273.

Shu, X.M., 2000b. Curculigo. In: Wu, Z.Y., Raven, P.H. (Eds.), Flora of China 24. Science Press and Missouri Botanical Garden Press, Beijing and St. Louis, pp. 271–273.

Sniderman, J.M.K., Jordan, G.J., 2011. Extent and timing of floristic exchange between Australian and Asian rain forests. J. Biogeogr. 38, 1445–1455.

Snijman, D.A., 2013. Plants of the Greater Cape Floristic Region 2: The Extra Cape Flora. Strelitzia 30. South African National Biodiversity Institute, Pretoria.

Snijman, D.A., Kocyan, A., 2013. The genus *Pauridia* (Hypoxidaceae) amplified to include *Hypoxis* sect. *Ianthe*, *Saniella* and *Spiloxene*, with revised nomenclature and typification. Phytotaxa 116, 19–33.

Stamatakis, A., 2014. RAxML version 8: a tool for phylogenetic analysis and post-analysis of large phylogenies. Bioinformatics 30, 1312–1313.

Stevens, P.F., 2001 onwards. Angiosperm Phylogeny Website. Version 14, July 2017 [and more or less continuously updated since].

Swofford, D.L., 2002. PAUP*: Phylogenetic Analysis Using Parsimony (*and Other Methods). Version 4. Sinauer Associates, Sunderland, Massachusetts.

Tanentzap, A.J., Brandt, A.J., Smissen, R.D., Heenan, P.B., Fukami, T., Lee, W.G., 2015. When do plant radiations influence community assembly? The importance of historical contingency in the race for niche space. New Phytol. 207, 468–479.

Uribe-Convers, S., Carlsen, M.M., Lagomarsino, L.P., Muchhala, N., 2017. Phylogenetic relationships of *Burmeistera* (Campanulaceae: Lobelioideae): combining whole plastome with targeted loci data in a recent radiation. Mol. Phylogen. Evol. 107, 551–563.

van Zinderen Bakker, E.M., Mercer, J.H., 1986. Major late Cainozoic climatic events and palaeoenvironmental changes in Africa viewed in a world-wide context. Palaeogeogr. Palaeoclimatol. Palaeoecol. 56, 217–235.

Verboom, G.A., Linder, H.P., Forest, F., Hoffman, V., Bergh, N., Cowling, R.M., 2014. Cenozoic assembly of the Greater Cape flora. In: Allsopp, N., Colville, J.F., Verboom, G.A. (Eds.), Fynbos: Ecology, Evolution and Conservation of a Megadiverse Region. Oxford University Press, Oxford, pp. 93–118.

Verboom, G.A., Linder, H.P., Stock, W.D., 2003. Phylogenetics of the grass genus *Ehrharta*: Evidence for radiation in the summer-arid zone of the South African Cape. Evolution 57, 1008–1021.

White, F., 1981. The history of the Afromontane archipelago and the scientific need for its conservation. Afr. J. Ecol. 19, 33–54.

Wiland, J., 1997. The genus *Curculigo* (Hypoxidaceae) in central Africa (Zaire, Rwanda, Burundi). Fragm. Flor. Geobot. 42, 9–24.

Wiland-Szymańska, J., 2001. The genus *Hypoxis* (Hypoxidaceae) in central Africa. Ann. Missouri Bot. Gard. 88, 302–350.

Wiland-Szymańska, J., 2002. Taxonomic and morphological notes on *Hypoxis angustifolia* (Hypoxidaceae) from Africa, Madagascar, and Mauritius. Novon 12, 142–151.

Yu, Y., Harris, A.J., He, S., 2010. S-diva (statistical dispersal-vicariance analysis): a tool for inferring biogeographic histories. Mol. Phylogen. Evol. 56, 848–850.

Zachos, J., Pagani, M., Sloan, L., Thomas, E., Billups, K., 2001. Trends, rhythms, and aberrations in global climate 65 Ma to present. Science 292, 686–693.